DLR Report

DLR-IB-AS-GO-2024-57

Lilium Pegasus outwash in hover

A.D. Gardner

Deutsches Zentrum für Luft- und Raumfahrt

Institute for Aerodynamics and Flow Technology

Deutsches Zentrum
DLR für Luft- und Raumfahrt

Deutsches Zentrum
für Luft-
und Raumfahrt e. V.

Institute for Aerodynamics
and Flow Technology
Göttingen

Report DLR-IB-AS-GO-2024-57

Author A.D. Gardner

Title **Lilium Pegasus outwash in hover**

Program : LEV
Customer : Lilium
Account : 3038140
Keywords : Outwash, Wake, Rotorcraft, eVTOL, Lilium, PAXMAN

Distribution : ■ I free ☐ II int. free ext. restricted ☐ III int. restricted ext. restricted ☐ IV confidential

Distribution: Digital only:
DLR-AS-HEL
Lilium

Report contains: 29 Pages incl.
4 Tables
13 References
31 Figures

Document source: Place: Göttingen
Department: AS-HEL-GÖ
Date: February 2024

Institute head	Department head	Author
Digital signiert von i. V. Andreas Dillmann Ort: Göttingen Datum: 2024.03.21 13:37:24+01'00'		Digital signiert von Anthony Gardner DN: PostalCode=51147, O=Deutsches Zentrum fuer Luft- und Raumfahrt e. V. (DLR), STREET=Linder Höhe, S=Nordrhein-Westfalen, C=DE, CN=Anthony Gardner, E=tony.gardner@dlr.de Grund: Ich bin der Verfasser dieses Dokuments Ort: Datum: 2024.03.21 12:50:03+01'00' Foxit PDF Editor Version: 13.0.1
Prof. Dr. A. Dillmann	Prof. Dr. M. Raffel	Dr. A.D. Gardner

Executive summary

This report analyzes the outwash of the 7-seat Lilium Pegasus (L4-100/MK12) (mass 3175 kg/wingspan 14 m), an electric VTOL jet, using electric ducted propellers with thrust vectoring, see Fig. 1. The outwash was computed by Lilium with an in-house CFD code, and the wake was analyzed by DLR for maximum velocity, PAXMAN forces and overturning moments, and compared with the Airbus H145 helicopter, which is similar in mass and passenger number.

The outwash from a single main rotor helicopter is approximately axisymmetric. The main rotor downwash is turned outward by the ground, forming an annular jet, reducing in strength with distance. The outwash can cause lifting, tipping or instability of persons or objects near the aircraft. Multirotor aircraft generate more outwash fore and aft of the aircraft and less outwash to the side of the aircraft. Maximum downwash velocity increases linearly with increasing aircraft mass, and decreasing rotor area. The shape of the Lilium jet outwash is qualitatively similar to that for tilt-wing aircraft.

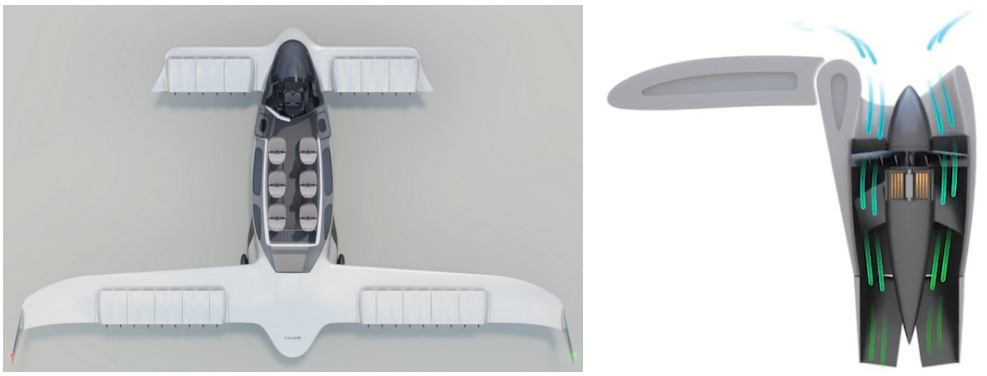

Figure 1: Lilium Pegasus + Lilium ducted rotor in hover configurations.

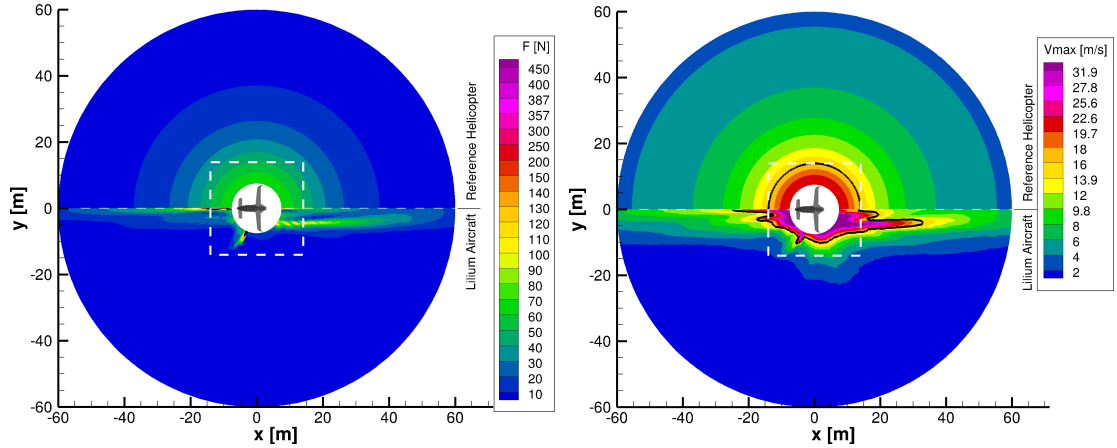

Figure 2: Force and V_{max} contours for hover height 5 m. Left: PAXMAN Forces with load limit 160 N as a black contour, Right: V_{max} with limit 16 m/s as a black contour.

In Fig. 2 the outwash shape is different for the Lilium jet (bottom) than for the helicopter (top). The white dashed square denotes the $2D$ cleared area around a landing pad. The outwash to the side has a low energy content compared to a helicopter outwash with the same maximum velocity. The PAXMAN force model for a civilian adult shows that, although high peak velocities were seen that these do not translate into forces of a worrying level for civilian personnel on the ground except for narrow jets in front of and behind the aircraft. Both of these levels are below the limits for trained personnel, and it seems unlikely that in the normal course of operations passengers would be in these areas. Except for the regions noted, the danger to persons outside the cleared area around a landing pad is similar to that for the comparable rotorcraft.

Contents

Abstract

This report is an analysis of the expected outwash effect of the Lilium Pegasus (L4-100/MK12) 7-seat variant (1 pilot/6 passengers), with take-off mass 3175 kg and wingspan of 14 m. Data is compared with a helicopter of similar capacity and mass, the Airbus H145. The outwash was computed by Lilium using their in-house CFD code, and the wake was analyzed by DLR for maximum velocity, PAXMAN forces and overturning moments. The shape of the Lilium jet outwash is qualitatively similar to that for tilt-wing aircraft, with jets fore- and aft of the aircraft. Except for the regions noted, the danger to persons outside the cleared area around a landing pad is similar to that for a comparable rotorcraft.

Nomenclature

a_0 .. a_{10}	Constants for the PAXMAN width equation (ft)
C_D	Drag coefficient (-)
f_y	Dimensionless velocity distribution for Preston's outflow model (-)
fy_{peak}	Shape constant for Preston's jet model (-)
$F_{pax}(r,\phi)$	PAXMAN force (N)
h	Vertical coordinate from ground (feet)
h_{max}	Outwash jet scaling height (m)
H	Hover height (m)
m	Aircraft mass (kg)
$M_{OBJ}(r,\phi)$	Moment (Nm)
ϕ=0:1:180	Azimuth (°)
r=7.5:2.5:60	Radius (m)
R	Rotor radius (m)
R_{min}	Radius of the rotor jet after contraction (m)
ρ	Density of air (kg/m^3)
$V(z,r,\phi)$	Flow velocity (m/s)
V_h	Mean velocity of the flow through the rotor plane (m/s)
V_{jet}	Velocity of the rotor jet after contraction (m/s)
V_{jetc}	V_{jet} modified for ground effect (m/s)
$V_{max}(r,\phi)$	Maximum velocity in the vertical direction (m/s)
$V_{peak}(r)$	Maximum velocity of outwash jet (m/s)
$V_{Preston}(z,r)$	Velocities from Preston's outflow model (m/s)
W	Width for the moment model (m)
$W_{pax}(z)$	Half-width distribution for the PAXMAN model (m)
z=0.01:0.01:2.01	Vertical coordinate from ground (m)

1 Introduction

The outwash from a single main rotor helicopter is expected to be approximately axisymmetric, with some second order effects due to trimming against the tail rotor and the fuselage shape. The mass flux processed by the main rotor to produce lift, flows downward (downwash), strikes the ground and is turned outward (outwash). These are sometimes referred to together as rotorwash. At its simplest, the outwash then forms an annular jet, which reduces in strength proportional to 1/distance from the jet center. This outwash can cause lifting, tipping or movement of loose objects, and tipping, pushing or instability of persons in the vicinity of the aircraft. The effect has long been well known, and is covered by many technical, theoretical and regulatory works. The mean outwash of classical single-rotor helicopters has been much studied, and at least for the outwash region away from the downwash can be estimated by a number of methods. Generally, the strength of a helicopter outwash increases linearly with increasing aircraft mass, and increases linearly with decreasing rotor area.

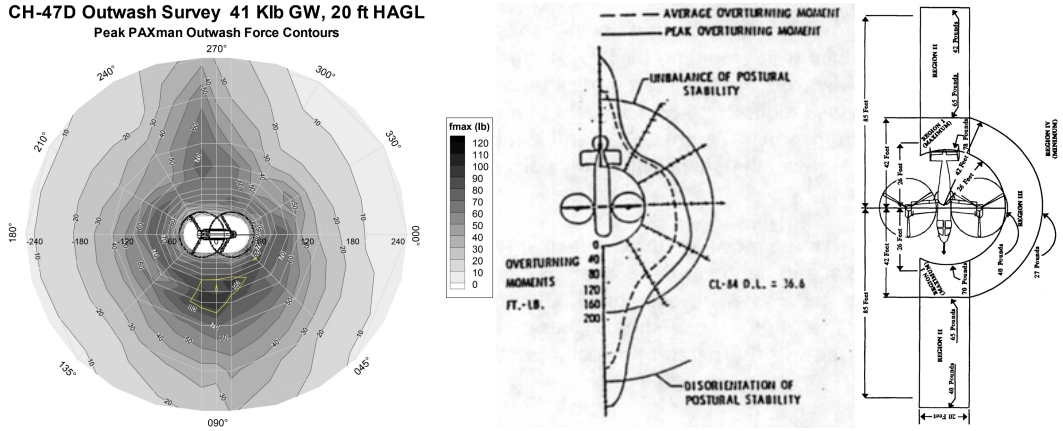

Figure 3: CH-47D [13], CL-84 [6] and XV-15 [5] outwash areas.

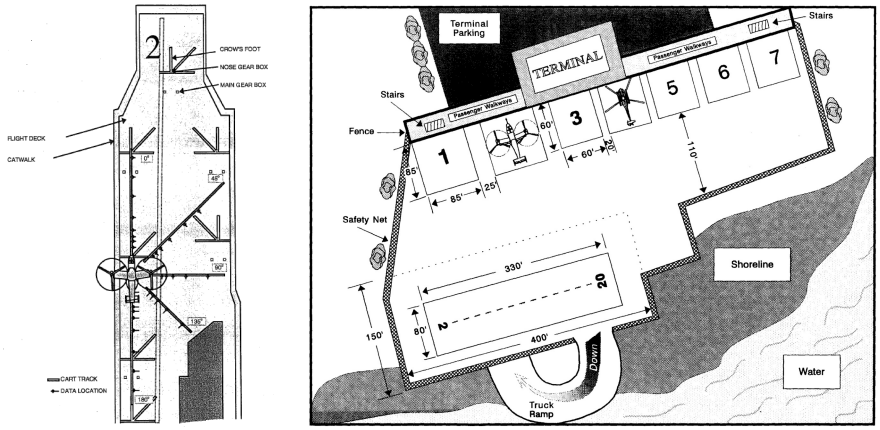

Figure 4: Left: V22 take-off/landing orientation on a carrier for outwash considerations [7], Right: Conceptual design for a full-service heliport [5], p.276.

In contrast, multirotor aircraft see a more complex shape, as seen in Fig. 3. For the CH-47D, the closely overlapping rotors generate ovoid contours of outwash force, punctuated by outward jets of higher outwash velocity where the rotors overlap. For tiltrotor configurations, including the CL-84 and the XV-15, the jet is toward the front and rear of the aircraft. In addition to this, tiltrotor aircraft have a relatively small "rotor" area, for the high aircraft mass, which will lead to large maximum downwash velocities. In contrast, any observers will be relatively far from the aircraft as measured in rotor diameters, so that the flow particularly to the side of the aircraft may be less at the same absolute distance in meters than for a helicopter of comparable mass. Particularly the CAA CAP 2576 [2] has recently drawn attention to the

potential differences between helicopter outwash and eVTOL outwash.

This kind of fore-and-aft outwash is part of rather standard considerations for landing tilt-wing aircraft on carrier decks, see Fig. 4, left. In equal part, it is also part of the design of conceptual ideas for heliports, as in the example in Fig. 4, right [5], where the landing area is oriented so that the fore-and-aft outwash will not impinge the parked aircraft or the passengers, and so that the take-off and landing direction is not over the passenger facilities. It will be seen in this report that the Lilium jet fits well into this kind of schema.

The Lilium jet is an electric vertical take-off and landing jet, see Fig. 5. It uses electric ducted propellers (Fig. 6), which can provide vectored thrust for VTOL or maneuvering. The propulsion units (30) are located on the top of the wing (18) and canard (12) trailing edge flaps, and are deflected 0° in cruise and 90° in hover. The rotors of the ducted propulsors have a radius of 15.5 cm. This document refers to the Pegasus (L4-100/MK12) 7-seat variant (1 pilot/6 passengers), with take-off mass 3175 kg and wingspan of 14 m. The canard (smaller of the two wings) is at the front of the aircraft.

The total area of the Lilium rotors is around 2.3 m^2, compared with 95 m^2 for the Airbus H145, a helicopter comparable in mass and passenger number. The air jet velocity at the duct exit can be expected to be considerably higher than that for the helicopter at the rotor plane, with the exact number depending on the duct geometry. The outwash thus has the potential to be more dangerous than that of a helicopter of comparable size.

Figure 5: Lilium 6-seat + Pilot configuration.

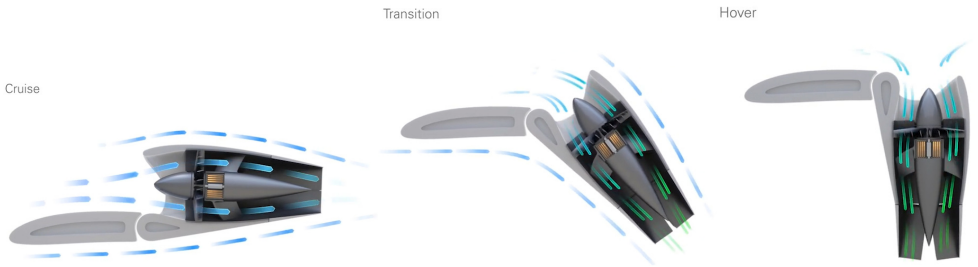

Figure 6: Lilium ducted rotor in cruise, transition and hover configurations.

Many authors (including [1] and the [11]) note both that the unsteady loads from a rotorcraft are important for the effect on ground personnel, and that the unsteady component of new configurations is not necessarily the same as for classical helicopter configurations [3]. For instance, the PAXMAN loading model distinguishes between mean and peak loads, where the limits for peak loads are expected from calibrations using existing helicopter measurements to be up to 130% of the mean loads. Similarly, measured data from currently flying aircraft (Fig. 7) shows the standard deviation of velocity to be in the range 30-60% of the mean velocity near the peak of velocity measured. The top row of Fig. 7 shows results from helicopters, with the CH-53E at 20 tonnes showing a 30-60% increase in peak compared to the mean. For the CH-53G at 14 tonnes a 25-35% increase in the peak is seen, whereas for the Bo105

with MTOW 2500 kg a standard deviation in the range 30-45% of the mean flow is seen. Braukmann et al. [1] also showed that the majority of the turbulent energy in the flow was in the <10 Hz range. For the two tiltwing aircraft in the bottom row of Fig. 7, standard deviations in the range 30-45% of the mean flow were also observed.

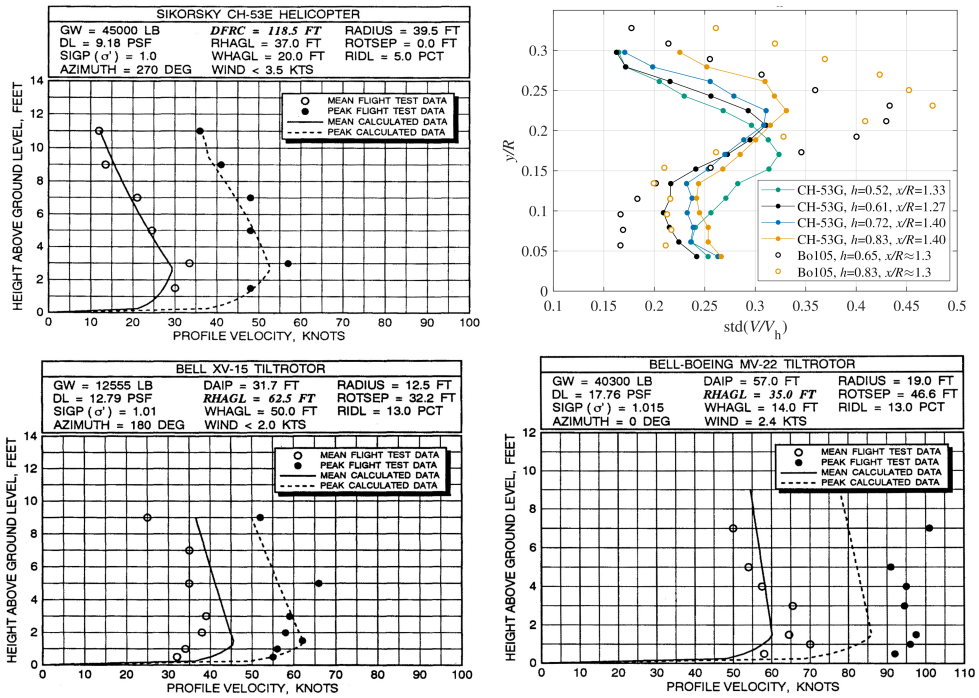

Figure 7: Unsteady outwash data from the literature: Top Left: CH-53E ([5](p.87)), Top Left: Bo105 and CH-53G ([1], Bottom Left: XV-15 ([5](p.111)), Bottom Left: MV-22 ([5](p.113)).

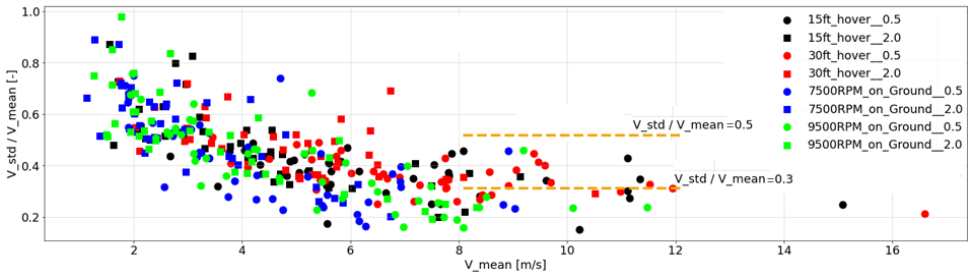

Figure 8: Unsteadiness of flow generated in Lilium Phoenix (5-seater) flight testing.

Flight test data of the Lilium Phoenix 5-seater prototype (1300 kg) was provided to the DLR from Lilium. During hovering flight, data was collected using 5-hole probes mounted on poles on the ground. For the purposes of this analysis only data from the center hole is considered, making it essentially a Pitot probe. An analysis of 28 different Probe positions around 14 poles with 2 heights (0.5 m and 2.0 m) allows insight into the unsteady component of the flow. For speeds >4 m/, where significant mean flow is present, the standard deviations are mostly in the range of 30-50% of the mean velocity, making it similar to that measured for helicopters, see Fig. 8. For this reason, it appears that the conclusions about velocity and force limits on personnel from helicopter wake investigations into the effect of the mean flow can be transferred to the Lilium jet, and that no particular changes due to the unsteady flow are to be expected.

This document provides an overview of the outwash analysis done by the DLR on data delivered by Lilium under an external contract. The analysis took place between December 2023 and February 2024.

2 Numerical method

Lilium performed a computational fluid dynamics (CFD) analysis using an in-house Reynolds-averaged Navier-Stokes (RANS) solver. No near-aircraft flow was provided to DLR, and this section reports details provided by Lilium about the CFD code. A half-grid was computed, symmetric around the aircraft midline, with the aircraft above the center of the ground plane, which was at x,y,z=0,0,0 m. Flow velocity was extracted from this solution in the outwash area at heights z=0.01:0.01:2.01 m, and at radii r=7.5:2.5:60 m and for azimuthal angles ϕ=0:1:180°, for a total of 800,832 points. DLR computed forces, moments and maximum velocity as 2-D fields and did analysis and illustration, see Fig. 9. All data and codes were provided from DLR to Lilium.

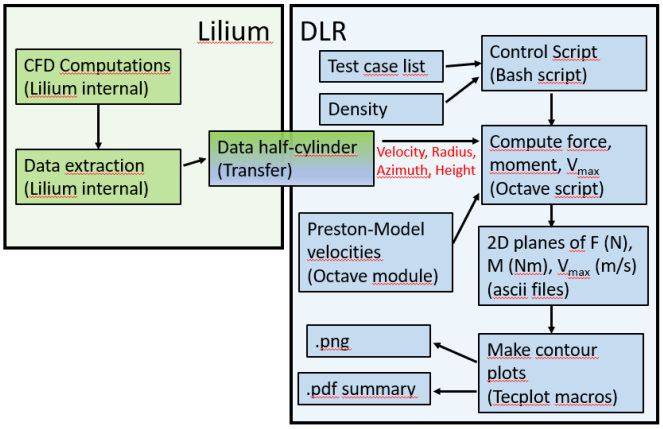

Figure 9: Flow chart of data handoff between DLR and Lilium, with analysis steps performed.

The CFD results are computed using Lilium's in-house CFD code, which is a 2nd order, unstructured code. The code uses an implicit RANS solver in this case with low Mach-number preconditioning. A k-omega SST turbulence model is used, with the Venkatakrishnan limiter. The aircraft is embedded within a farfield at 20 aircraft lengths. A starting mesh pre-refinement box (r=50 m, h=2 m) is used (see Fig. 10). During the computation, adaptive mesh refinement (AMR) at 3 cm is used to refine the region between the aircraft and the ground, and the jet region, so that the velocity gradients are transported as expected. The engines are modelled using a pressure-outlet boundary with target mass flow rate at the inlet, with a mass flow boundary defined with total temperature at the outlet. An adiabatic no-slip wall is defined for the ground, with constant roughness height of 50 mm. The aircraft is trimmed by setting the engine mass flow.

The DLR assessment of this modeling is that this approach has a very good likelihood of correctly capturing the mass and momentum flow through the engines. It is not entirely clear whether the velocity fields in the outwash area will be more spread out in the CFD than in reality due to diffusion in the grid, or more concentrated due to the CFD not considering the turbulent mixing at the ground plane. However, it seems likely that the integral methods will be better matched by the CFD than the peak velocity values.

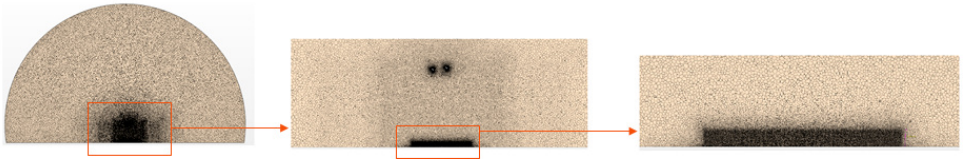

Figure 10: Grid pre-refinement region before adaptive mesh refinement (side view) at three zoom levels.

3 Preston's helicopter outwash model

In this report the Lilium jet outwash computed with CFD is contrasted with the outwash of a comparable helicopter, the Airbus H145, also known as the UH-72 Lakota. This is (depending on variant) a 6-person (plus pilots) aircraft with an assumed mass for these computations of m=3600 kg. The rotor radius is R=5.5 m, and it is assumed to be hovering with the rotor $\frac{H}{R} = 0.8$ rotor radii over the ground.

The outwash model of Preston (1994) [10] is used by our group at DLR, as seeming to have a good agreement with measured data, as will be seen at the end of this section. The model itself requires knowing the maximum velocity in the rotor downwash jet after contraction (V_{jetc}), and the radius of the jet after contraction ($R_{min} = R/\sqrt{2}$). All other values are scaled according to these.

The downwash at the rotor plane is computed from the aircraft mass and the rotor radius as:

$$V_h = \sqrt{9.8m/(2\rho\pi R^2)} \tag{1}$$

and is usually called the hover-induced velocity. The maximum velocity after jet contraction (V_{jet}) can be a maximum of $2V_h$, but V_h is reduced by ground effect for low hover heights (H)

$$V_{jetc} = (1 - 0.9exp(-2\frac{H}{R})) \cdot 2V_h \tag{2}$$

Preston's model scales the distance from the rotor center with the minimum radius after wake contraction r/R_{min}, rather than the rotor radius r/R used by many other authors, leading to a distance difference which must be corrected if scaling with R:

$$\frac{r}{R_{min}} = \frac{\sqrt{2}r}{R} \tag{3}$$

Preston's model computes a vertical velocity profile which varies with radius from the helicopter (r), and is scaled in its maximum velocity (V_{peak}) and stretched in height (h_{max}) depending on the helicopter dimensions. The maximal radial velocity is computed using Eqn. 6 from [10]:

$$V_{peak} = V_{jetc}\frac{r}{R_{min}}/1.25 \qquad \frac{r}{R_{min}} < 1.25 \tag{4}$$

$$V_{peak} = V_{jetc} \qquad \frac{r}{R_{min}} < 2.83 \tag{5}$$

$$V_{peak} = 2.83V_{jetc}/\frac{r}{R_{min}} \qquad \frac{r}{R_{min}} > 2.83 \tag{6}$$

The shear layer height is then computed using Eqn. 14 from [10], using some calibration constants which have been somewhat simplified here:

$$fy_{peak} = 0.187 \tag{7}$$

In this model h_{max} does not depend on the aircraft height:

$$h_{max} = \frac{R}{\sqrt{2}} \qquad \frac{r}{R_{min}} < 2.83 \tag{8}$$

$$h_{max} = \frac{R}{\sqrt{2}}\frac{r}{R_{min}}/2.83 \qquad \frac{r}{R_{min}} > 2.83 \tag{9}$$

The dimensionless height function is then computed using [10] Eqn. 4:

$$f_y = \left(\frac{h}{h_{max}}\right)^{\frac{1}{2}}\left(1 - \frac{h}{h_{max}}\right)^5 \tag{10}$$

and this is dimensionalized, giving a velocity function (m/s) for all radii:

$$V_{Preston} = V_{peak} f_y / f y_{peak} \tag{11}$$

Preston's model is validated against measured jet velocity from the DLR in Fig. 11. Varying the helicopter take-off mass between 2.5 tonnes (Bo105) and 14 tonnes (CH-53G) does not affect the model scaling, and that the agreement is good up to distances of $6.4R$ (35 m), which is the greatest distance for which we have data. It will be seen later that no significant danger to ground personnel is expected at distances greater than this.

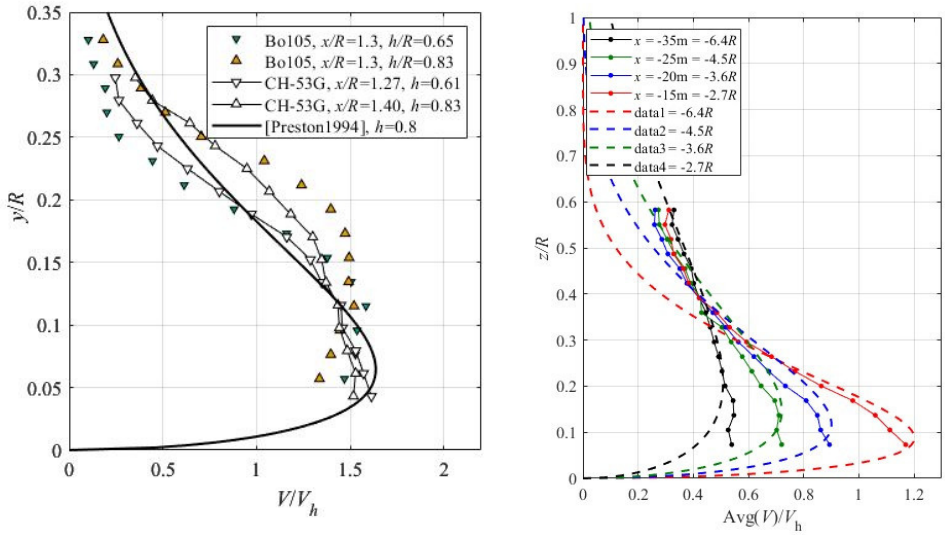

Figure 11: Validation of Preston model flow velocity (lines) against experimental data for single main rotor helicopters (Left) close to the helicopter (Right) further from the helicopter.

4 PAXMAN force model

The PAXMAN force model is an integral force model which computes the force in Newtons over a person-like shape with an area of 0.543 m^2, see Fig. 12, defined by the half-width distribution W_{pax}:

$$\frac{W_{pax}}{0.3048} = a_0 + a_1 h + a_2 h^2 + a_3 h^3 + a_4 h^4 + a_5 h^5 + a_6 h^6 + a_7 h^7 + a_8 h^8 + a_9 h^9 + a_{10} h^{10}; \quad (12)$$

where the height (h) is in feet and the width W_{pax} is in meters. The coefficients are found in Fig. 12.

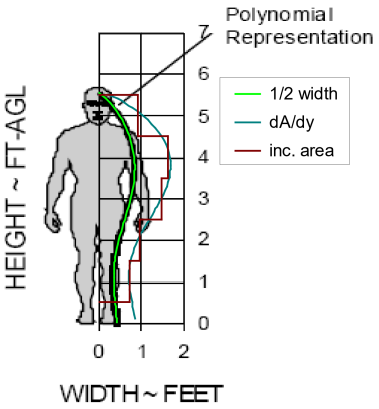

a_0	4.31e-01
a_1	-4.64e-02
a_2	-1.40e-01
a_3	1.37e-01
a_4	-0.0248764
a_5	-5.50e-04
a_6	2.22e-04
a_7	-4.18e-05
a_8	1.45e-05
a_9	-7.80e-08
a_{10}	-1.90e-07

Figure 12: PAXMAN coefficients with units in feet, as listed in [5](p.158). a4 appears to be false in Rovere [12] but correct in Silva [13] and older. Preston [10] falsely notes it is a power 9 series.

At each (r,ϕ) point the force is obtained by integrating the velocity distribution in the z-direction:

$$F_{pax} = C_D \sum_{z=0}^{z=2m} \frac{1}{2} \rho V^2 \cdot 2W_{pax} \cdot \Delta z \quad (13)$$

where z is the height above the ground plane in meters, $V(z,r,\phi)$ is the flow velocity and C_D=1.0 is the drag coefficient of the shape. The width of the shape is multiplied by two to have the full width.

The relevant limits are defined by [9], as listed in [11], see Tab. 1

Type	Force limit
Caution, Military (mean)	80-87 lbf (356-387 N)
Caution, Military (peak)	87-115 lbf (387-512 N)
Hazard, Military (mean)	>87 lbf (387 N)
Limit, Civilian (mean)	180 N

Table 1: Force limits for the PAXMAN model [11].

As mentioned above, the Lilium jet does not display any special behavior regarding the unsteady loads when compared with a helicopter, so that the mean loads can be taken as a guideline. The “Rotorwash Analysis Handbook” [5] lists other models for personnel, and for those the limit is taken as half of the caution for military personnel. For the purpose of this study the load limit for the PAXMAN model is taken to be 180 N.

5 Velocity models

The maximum velocity V_{max} at each radial and azimuthal position is the simple maximum of the velocities in the range 0 m$< z <$2 m. Velocity is often used as a proxy for force, since it is more easily estimated in historical data or incident analyses. The "Rotorwash Analysis Handbook" [5] identifies the range 30-37 knots (15-19 m/s) as a critical range for the interaction with parked rotorcraft, 30-40 knots (15-20 m/s) as a critical range for motorcycles, 43-47 knots (22-24 m/s) for oil drums. Additionally, for damage to door cowlings the range 30-37 knots (15-19 m/s) is identified as critical. From the EASA document "PTS VPT-DSN.C.230 Downwash protection", and a table from the Australian CAA, 60 km/h ($\approx$16.7 m/s) wind speed is identified as a limit for civilian operations. For this report 16 m/s is taken to be the limit of concern, for direct aerodynamic effects of the wake.

Additionally, lifted particulates (usually identified as sub-2 mm corns) cause engine damage if the wake flow causes them to be reingested, paint and surface damage when thrown against vehicles and structures, and can pose a hazard to vision (brownout/whiteout). These indirect aerodynamic problems are additional to the discussion in this document. Masters et al. [8] gives an estimate of gravel particle sizes which will be directly lifted from a roof or ground, which is probably a good estimate for a limit of the size of objects which can be directly lifted (rather than pushed or tipped) by the outwash further from the aircraft, see Tab. 2. The chosen limit of 16 m/s will lift 2-5 gravel, but mostly not 8-16 stones (small garden bed pebbles).

Diameter (mm)	Threshold of flight (m/s)
2.4	9.8
4.75	13.9
9.5	19.7
12.5	22.6
16	25.6
19	27.8
25	31.9

Table 2: Pick-up speeds for gravel [8].

6 Moment models

The moment model in this report is from the "Rotorwash analysis Handbook" section 5.1.2 [5]. It follows essentially the same logic as the PAXMAN model, that there is an area with a width-height distribution which is acted upon by the dynamic pressure of the outwash. As shown in Tab. 3, the assumption is that the object is a rectangle of constant width, and that the drag coefficient varies with the type of object. In contrast to the PAXMAN model, the moment models list both a force and a moment around a hinge at ground level to model tipping, where the moment is computed by Eqn. 14. The limits listed in [5] are shown in Tab. 4.

$$M_{OBJ} = C_D \sum_{z=0}^{z=Height} \frac{1}{2}\rho V^2 \cdot W \cdot z \cdot \Delta z \tag{14}$$

Type	Large	Small	55 Gal (200 L) Drum	Motorcycle
Height	1.83 m	1.22 m	0.89 m	0.88 m
Width	0.34 m	0.24 m	0.58 m	1.83 m
C_D	1.1	1.1	0.65	0.5

Table 3: Personnel model from [5].

Type	Force limit	Moment limit
Trained Personnel	80 lbf	260 ft-lb (352 Nm)
Untrained Passengers	40 lbf	120 ft-lb (163 Nm)
Children (Type S)	30 lbf	60 ft-lb (81 Nm)
Drum (Empty)		30 ft-lb (41 Nm)
Drum (Medium)		70 ft-lb (95 Nm)
Motorcycle (Away from Stand)		66 ft-lb (89 Nm)
Motorcycle (Toward Stand)		117 ft-lb

Table 4: Force and moment limits for the moment models [5] (p.174, and pp.237/238).

The moment limits were computed for civilian adults and children as 160 Nm and 80 Nm respectively. The report "Rotorwash Operational Footprint Modeling" [11] goes into considerable detail about the effect of outwash on different objects, noting that light unsecured objects (tents) may be affected at very large distances, and that the modeling for drums, logs and motorcycles appears limited in its reliability, due to considerable variance in the actual objects encountered. It is noted that small, low density objects like bark mulch for gardens is subject to considerable lifting under rotor wash. Thus, the analysis that a person is not subject to overturning still requires a cleared landing area.

7 Results

Hover simulations were performed for hover heights 0 m to 20 m with the aircraft aligned along the x-axis (pointing to the left) and without sidewind. As seen in Fig. 13 (left) the distribution of maximum velocity qualitatively matches the expectation from tiltrotor aircraft. That is, that the velocity to the fore and aft of the aircraft is higher than the velocity to the side of the aircraft. The black contour line is the 16 m/s limit and this is compared to the cleared area of a nominal helipad (28 m x 28 m), shown as the dotted white box. From the EASA guidelines [4] protection, this cleared area should be two times the "rotor diameter" or in this case two times the wingspan. The area affected by the high-velocity jet is increased compared to the reference helicopter to the fore and aft, but decreased compared to the reference helicopter over the full range of sideward angles. This is supported by comparing the extracted velocity profiles at 15 m from the aircraft in Fig. 13 (right), where only a single profile is shown for the helicopter flow due to its axisymmetry. Forward of the aircraft (x=-15), the velocity distribution is rather similar to that for the helicopter, whereas aft (x=+15) the velocities are significantly higher. At the side of the aircraft (y=-15), the velocities are significantly lower.

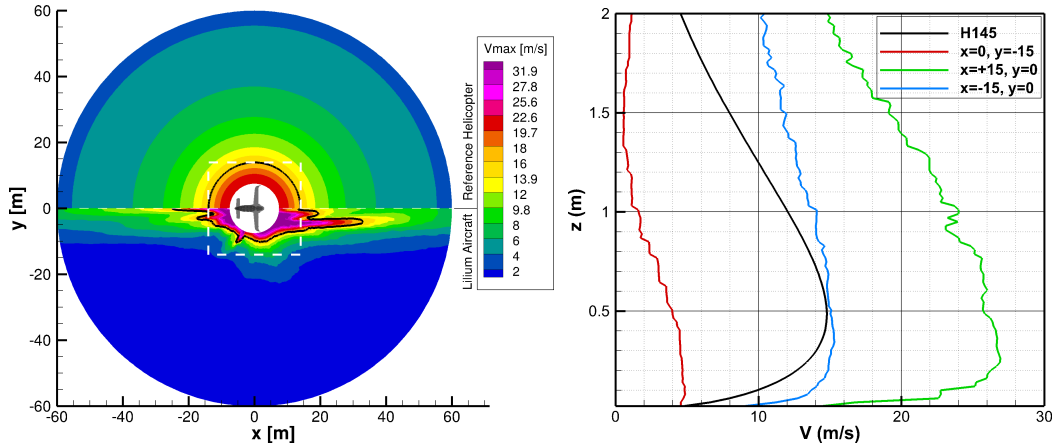

Figure 13: Velocity results for hover height 5 m. Left: V_{max}, Right: Velocity profiles at 15 m distance.

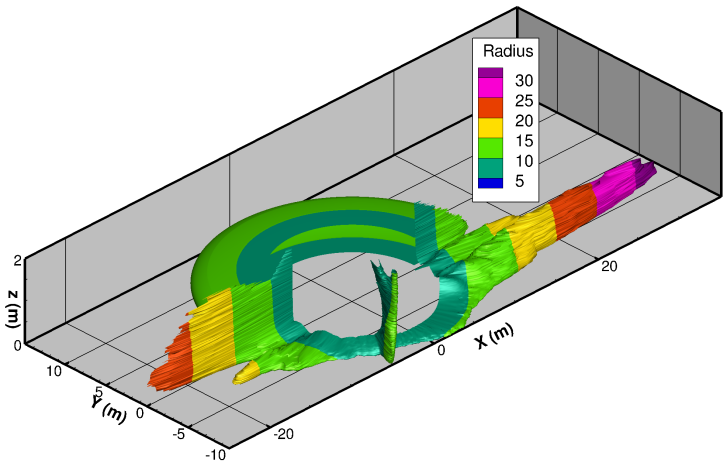

Figure 14: 3D isosurface at 16 m/s for hover height 5 m. The z-axis is scaled by a factor 6.

As shown in Fig. 14, the shape of the outwash is also different for the Lilium jet than for the helicopter, with flatter velocity distributions in the fore and aft jets. The outwash to the side is rather flat to the ground, so that the energy content is low compared to a helicopter outwash with the same maximum velocity. An additional jet at 45° towards the front is also visible, which is caused by the interaction between the canard and main wing jets at the ground plane. This 45° jet is stronger for some individual test cases, see Appendix B. Outside the predictive scope of this document is the high velocity level close

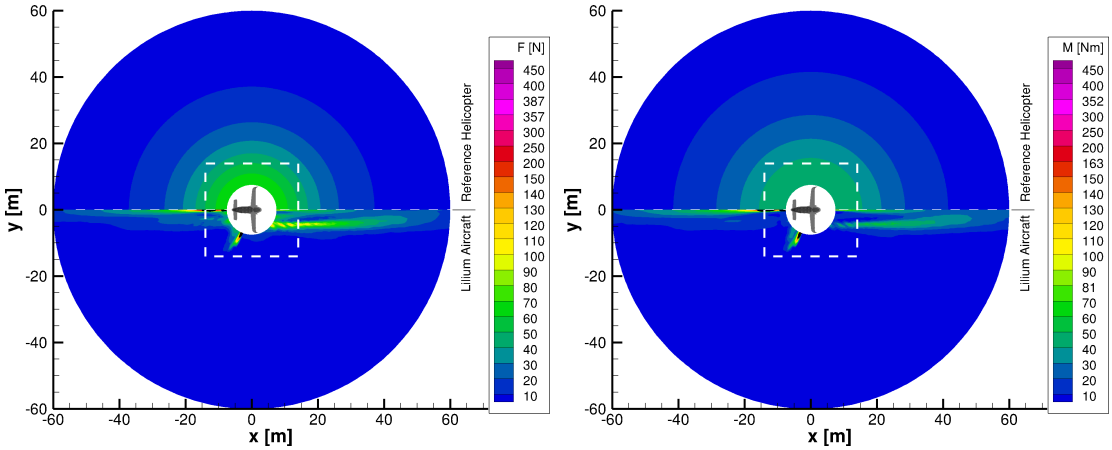

Figure 15: Force and moment contours for hover height 5 m. Left: PAXMAN Forces with limit 160 N, Right: Moment model for a civilian adult with limit 160 Nm.

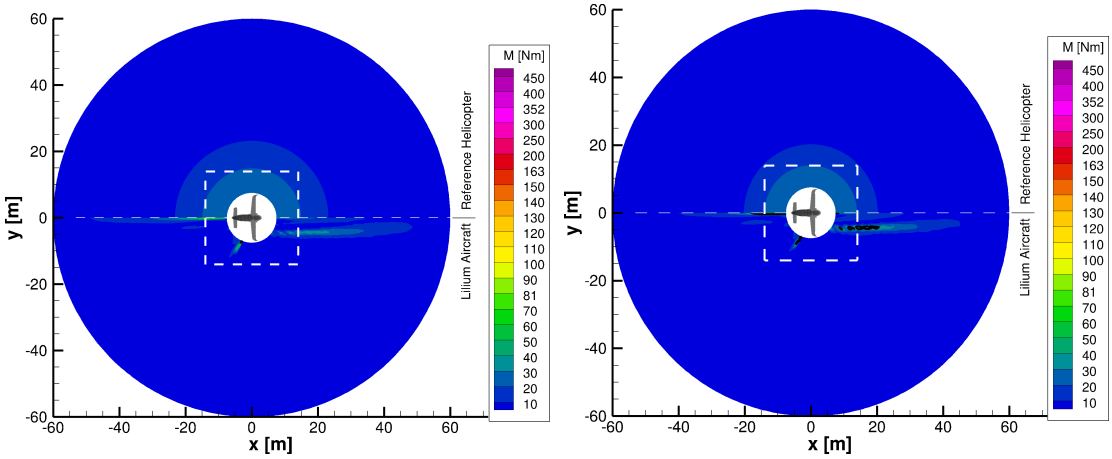

Figure 16: Moment contours for hover height 5 m. Left: Small person with limit 80 N, Right: Empty 200 L drum limit 41 Nm.

to the aircraft, which in theory could cause stones above 25 mm in diameter (see Tab. 2 and similar objects to become airborne and travel outside of the high-velocity area. Realistically, a few minutes of flight testing with the final aircraft should suffice to quantify the risk.

As the peak velocity is subject to higher uncertainty due to the modeling, the PAXMAN forces and the moment model for a civilian adult were computed and shown in Fig. 15. For the lilium jet in the bottom half of the images, the high peak velocities (Fig. 13) do not translate into forces or moments of a worrying level for civilian personnel on the ground except for narrow jets in front of the aircraft and at 45° forward. It must be emphasized that both of these levels are below the limits for trained personnel, and it seems unlikely that in the normal course of operations passengers would be in these areas. To the side of the lilium jet, both the force and moment levels are lower than for the reference helicopter. The moment model for a child, see Fig. 16, left, follows the results for an adult, since although the limit is lowered, the area is also reduced. In fact, the only object investigated which showed significant area with a danger of overturning was the empty 200 L drum, see Fig. 16, right.

The full set of results for hovering test cases are available in Appendix A. In general, the outwash becomes more symmetric and less strong as the aircraft ascends, and the maximum of asymmetry is visible close to the ground. Fig. 17 shows that for hovering at 20 m height, the V_{max} contours are more "helicopter-like". For 1.0 m hover height (Fig. 17) a long, thin area of high V_{max} on the axis of the aircraft is generated. Thus, it is probably advisable to land the aircraft so that persons, structures and

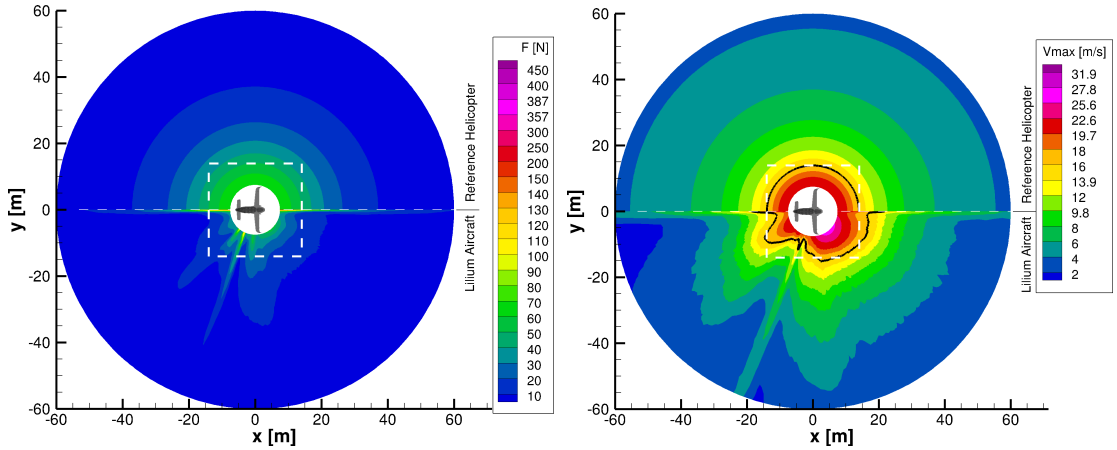

Figure 17: Contours for hover height 20.0 m, Left: PAXMAX forces, Right: V_{max}.

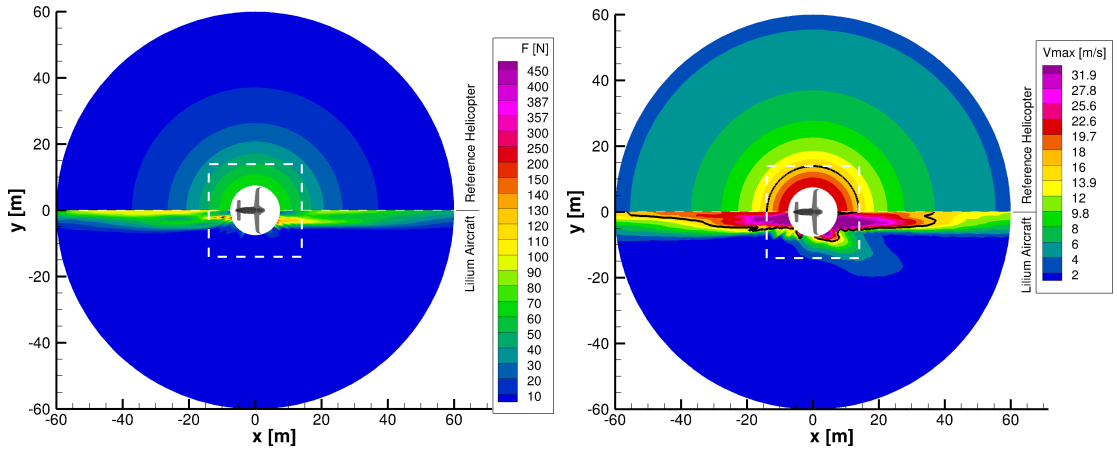

Figure 18: Contours for hover height 1.0 m, Left: PAXMAX forces, Right: V_{max}.

other aircraft are to the side of the landing aircraft. The PAXMAN or moment limits are not further exceeded by other hovering heights, as seen in Appendix A. It should be emphasized that the landing is a highly dynamic operation, which takes on the order of 10 seconds. It will take some seconds at a constant flight condition for the steady flow situation (as in the simulations) to be established.

After investigating a large test matrix of trim, wind, mass flow rate and dynamic take-off points, no special points of interest were found. The few points which may be interesting as corner cases for the flight envelope are in Appendix B.

8 Conclusions

This report is an analysis of the expected outwash effect of the Lilium Pegasus (L4-100/MK12) 7-seat variant (1 pilot/6 passengers), with take-off mass 3175 kg and wingspan of 14 m. Data is compared with Preston's wake model for a helicopter of similar capacity and dimensions, the Airbus H145. Comparisons of the unsteady component of the outflow for flight measurements of the 5-seater Lilium Phoenix showed similar levels of unsteadiness as for existing aircraft. The outwash was computed by Lilium using their in-house CFD code, and the wake of both the Lilium jet and the helicopter was analyzed by DLR for maximum velocity, PAXMAN forces and overturning moments. The shape of the Lilium jet outwash is qualitatively similar to that for tilt-wing aircraft, with jets fore- and aft of the aircraft. The fore-and-aft regions have an additional danger of objects uplifting (gravel etc.) compared to the helicopter outwash in those regions. The direct aerodynamic danger of tipping or pushing for persons outside the $2D$ cleared area around a landing pad is similar to that for a comparable rotorcraft.

9 Acknowledgements

For further questions, the contact persons for this contract were:
DLR AS-HEL: Anthony Gardner, Christian Wolf
Lilium: Tansu Sevine, Nele Bittel, Marvin König, Dominique Decard

References

[1] Braukmann, J.N., Schwarz, C., Wolf, C.C., Buron, E., Koch, S., Buske, G., Gardner, A.D., "BOS and Hot-Film Analysis of a CH-53G Helicopter Wake in Ground Effect", Vertical Flight Society 79th Annual Forum, West Palm Beach, Florida, May 16-18, 2023. DOI: 10.4050/F-0079-2023-18181

[2] Brown, R., "Understanding the downwash/outwash characteristics of eVTOL aircraft", CAA CAP 2576A, Civil Aviation Authority (CAA), 2023.

[3] Caprace, D.-G., Diaz, P.V., Yoon, S., "Simulation of the rotorwash induced by a quadrotor urban air taxi in ground effect", VFS 79th annual forum, West Palm Beach, May 6-8. 2023. DOI: 10.4050/F-0079-2023-17974

[4] EASA, "Certification Specifications and Guidance Material for the design of surface-level VFR heliports located at aerodromes that fall under the scope of Regulation (EU) 2018/1139", CS-HPT-DSN, Annex to ED Decision 2019/012/R, Issue 1, 23 May 2019.

[5] Ferguson, S. W., "Rotorwash Analysis Handbook, Volume I Development and Analysis", Federal Aviation Administration, Washington D.C., Technical Report DOT/FAA/RD-93/31,I, June 1994.

[6] Harris and Simpson, "CL-84 Tilt-Wing Vertical and Short Takeoff and Landing Downwash Evaluation", NATO SY-52R-76, April 1976

[7] Lake, R. E., "Shipboard V-22 Rotor Downwash Survey," NAWCADPAX-99-87-RTR, September 1999.

[8] Masters, F., and Gurley, K., "Performance of Embedded Gravel Roof Systems in Extreme Wind Loading," Department of Civil and Coastal Engineering, University of Florida, March 18, 2008.

[9] NAWCAD Patuxent River Report No. NAWCAD/4.6.5.5/2008-003, "Human Limits in Rotor Craft Downwash/Outwash", 18 Apr 2008.

[10] Preston, J.R. "VTOL Downwash / Outwash Operational Effects Model" AHS 50th annual forum, Washington May 11-13, 1994.

[11] Preston, J. R., Troutman, S., Keen, E., Silva, M., Whitman, N., Calvert, M., Cardamone, M., Moulton, M., and Ferguson, S. W., "Rotorwash Operational Footprint Modeling," Tech. rep., Missile Research Development and Engineering Center Redstone Arsenal AL Missile Guidance directorate, 2014.

[12] Rovere, F., Barakos, G. N. and Steijl, R. "Safety analysis of Rotors in Ground Effect", AIAA Aviation, 2-6 Aug 2021. DOI:10.2514/6.2021-2625

[13] Silva, M. J., "CH-47D Tandem Rotor Outwash Survey", NAWCADPAX/EDR-2010/120, August 2010.

10 Appendix A: Hover test cases

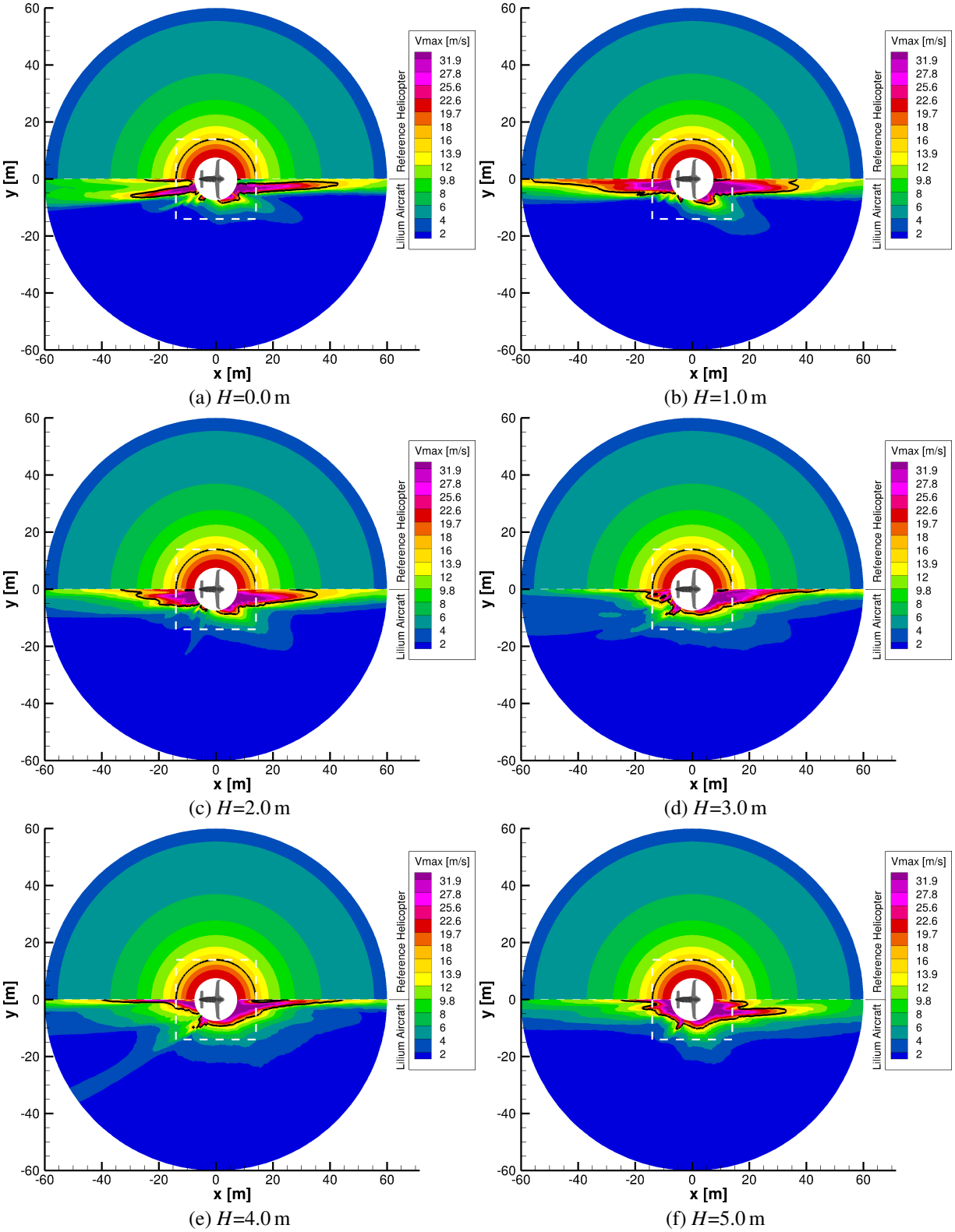

(a) H=0.0 m (b) H=1.0 m

(c) H=2.0 m (d) H=3.0 m

(e) H=4.0 m (f) H=5.0 m

Figure 19: V_{max} results for different hovering heights (1).

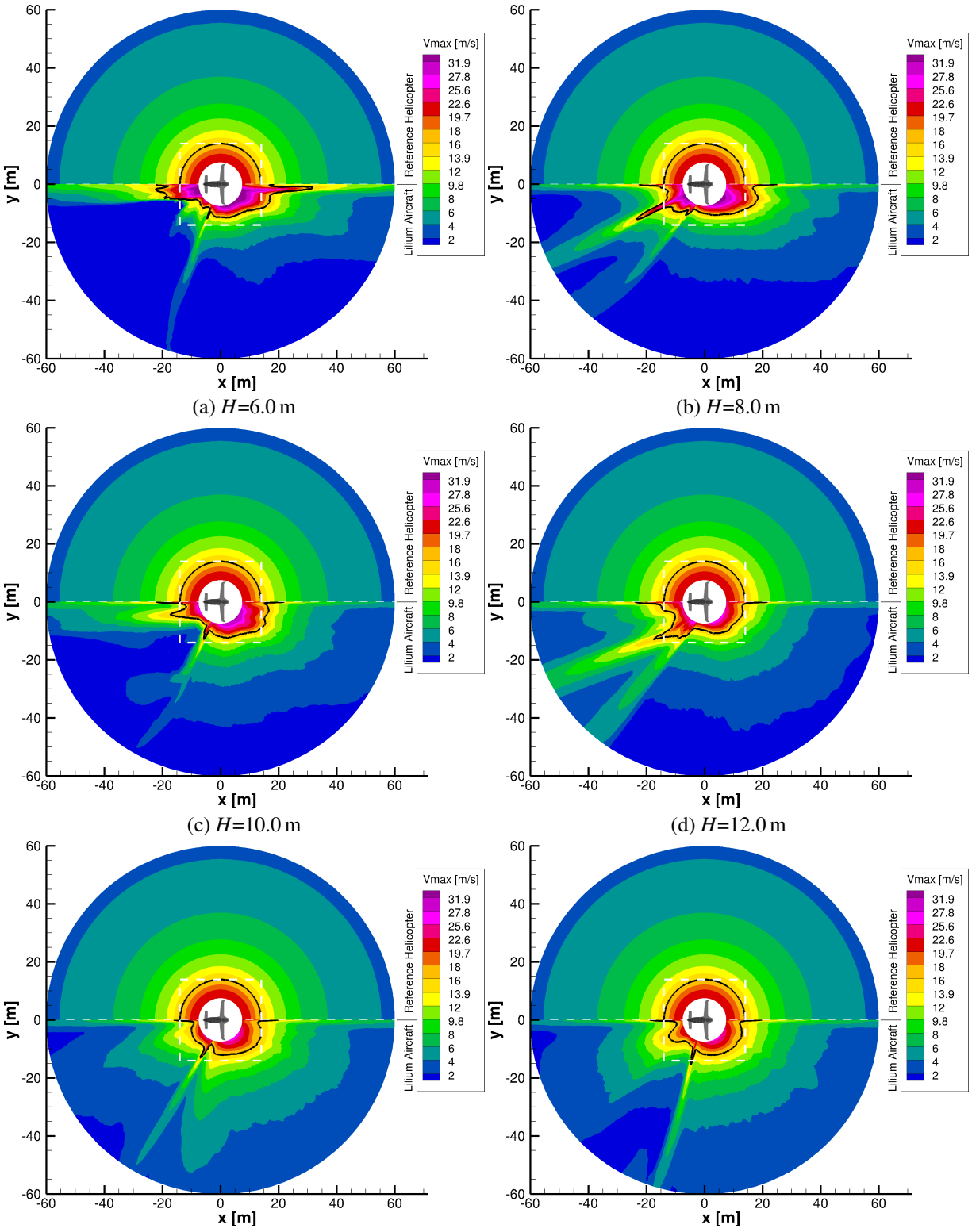

(a) H=6.0 m (b) H=8.0 m

(c) H=10.0 m (d) H=12.0 m

(e) H=14.0 m (f) H=16.0 m

Figure 20: V_{max} results for different hovering heights (2).

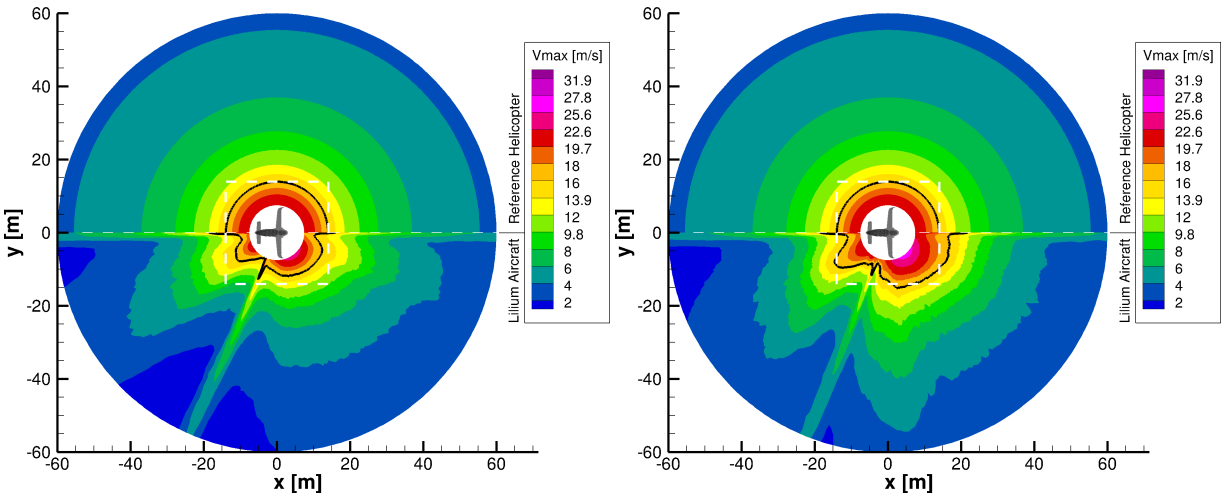

(a) H=18.0 m (b) H=20.0 m

Figure 21: V_{max} results for different hovering heights (3).

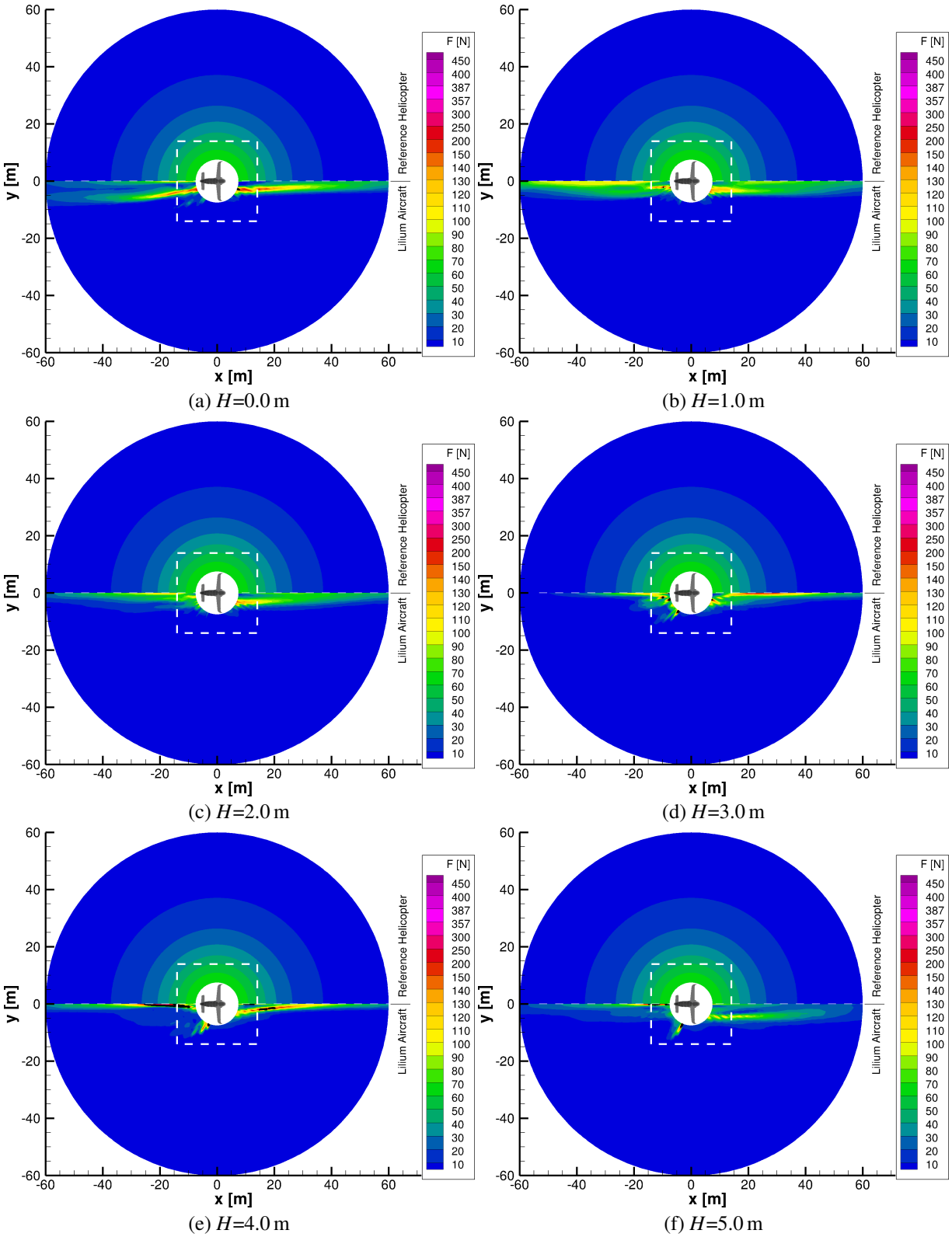

(a) H=0.0 m (b) H=1.0 m

(c) H=2.0 m (d) H=3.0 m

(e) H=4.0 m (f) H=5.0 m

Figure 22: PAXMAN results for different hovering heights (1).

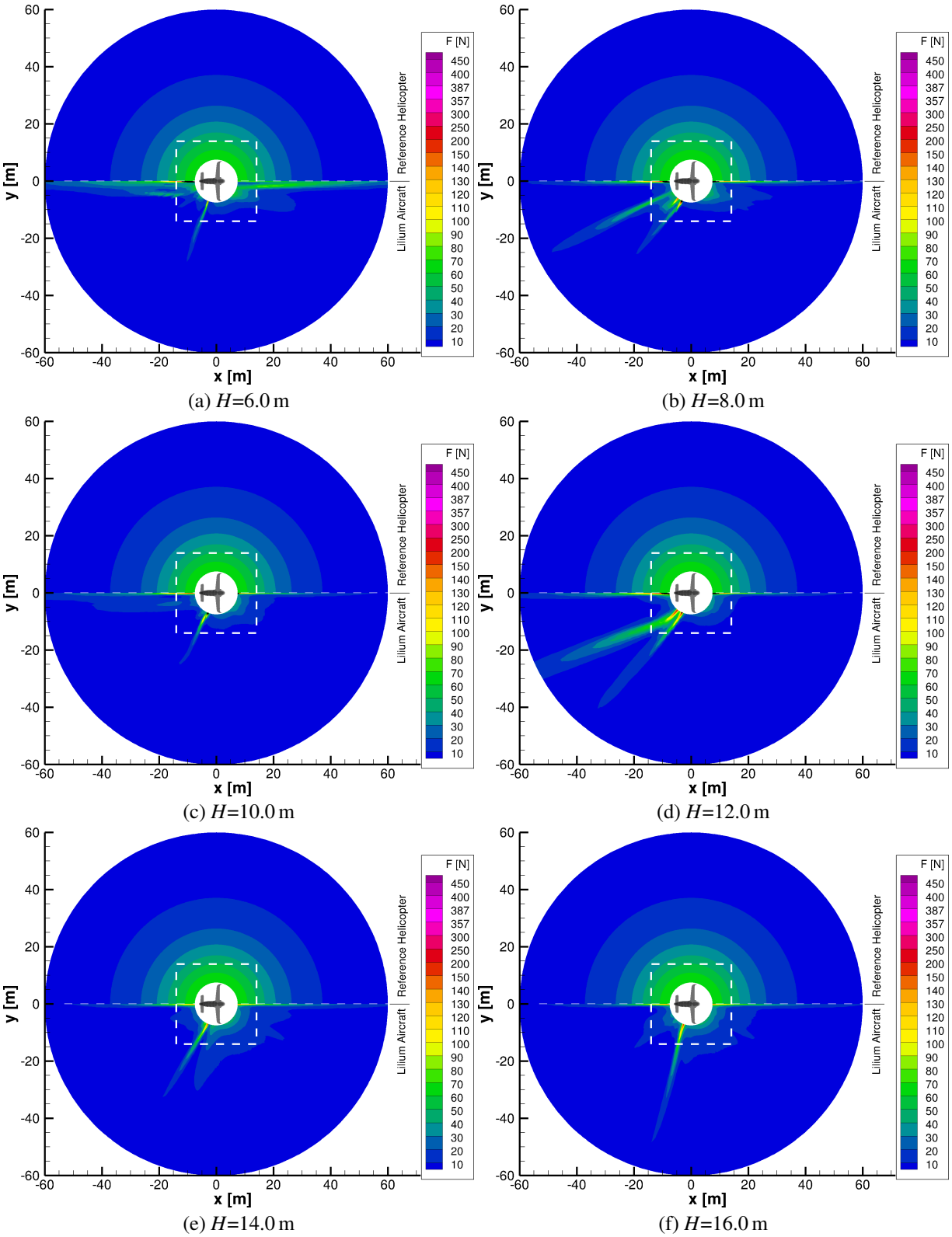

(a) H=6.0 m (b) H=8.0 m

(c) H=10.0 m (d) H=12.0 m

(e) H=14.0 m (f) H=16.0 m

Figure 23: PAXMAN results for different hovering heights (2).

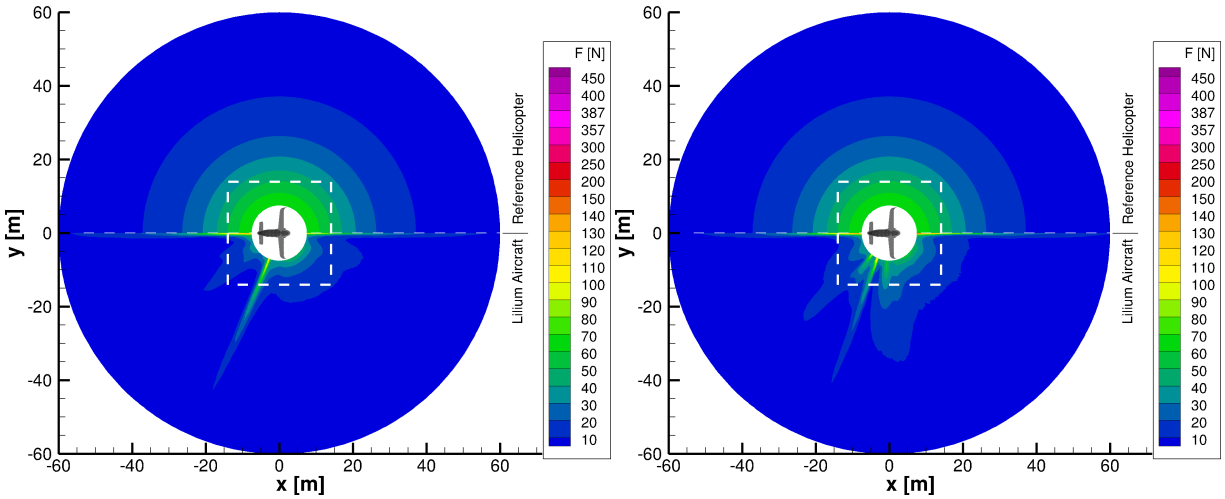

(a) H=18.0 m (b) H=20.0 m

Figure 24: PAXMAN results for different hovering heights (3).

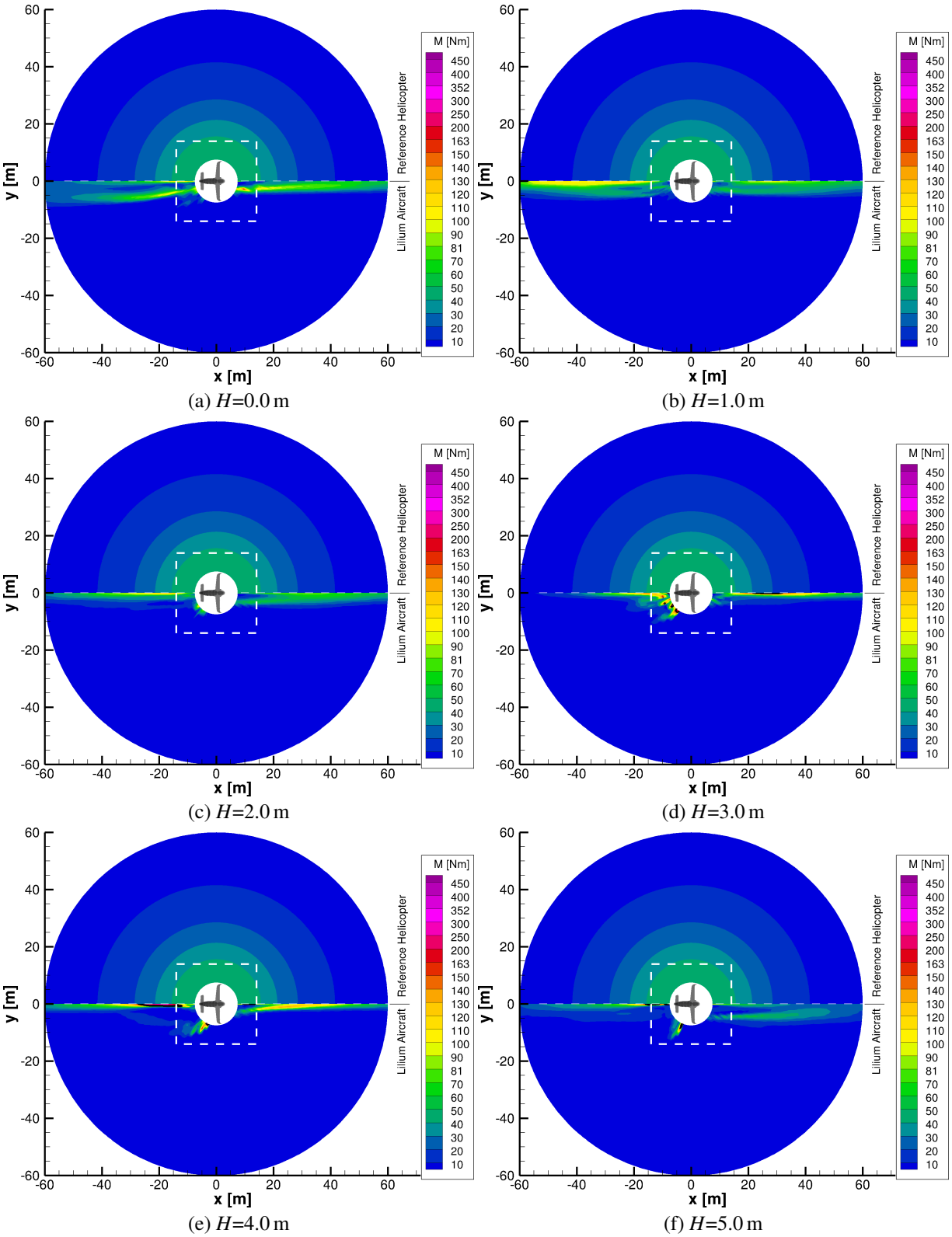

(a) H=0.0 m (b) H=1.0 m

(c) H=2.0 m (d) H=3.0 m

(e) H=4.0 m (f) H=5.0 m

Figure 25: Overturning moment for an adult civilian: results for different hovering heights (1).

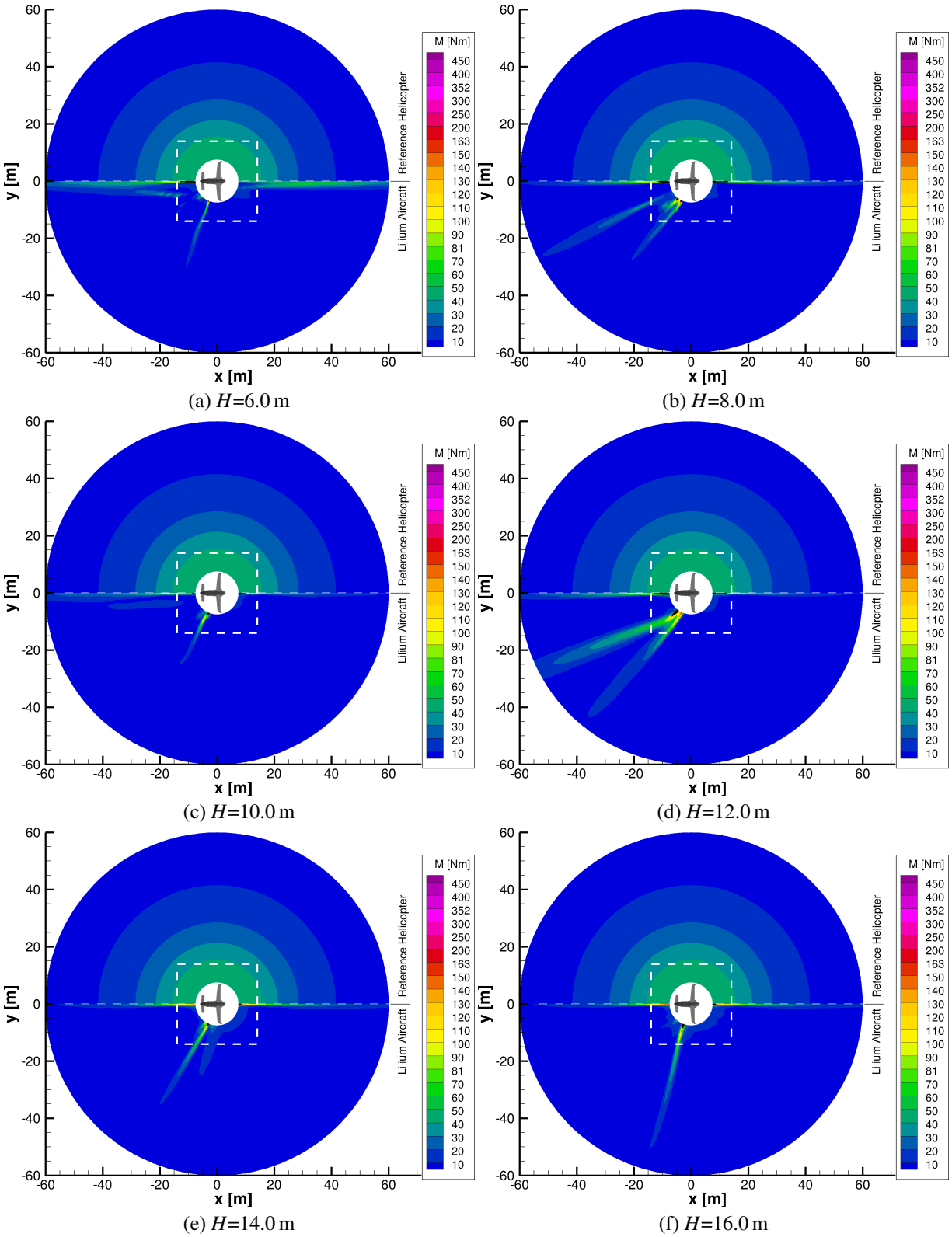

(a) H=6.0 m (b) H=8.0 m

(c) H=10.0 m (d) H=12.0 m

(e) H=14.0 m (f) H=16.0 m

Figure 26: Overturning moment for an adult civilian: results for different hovering heights (2).

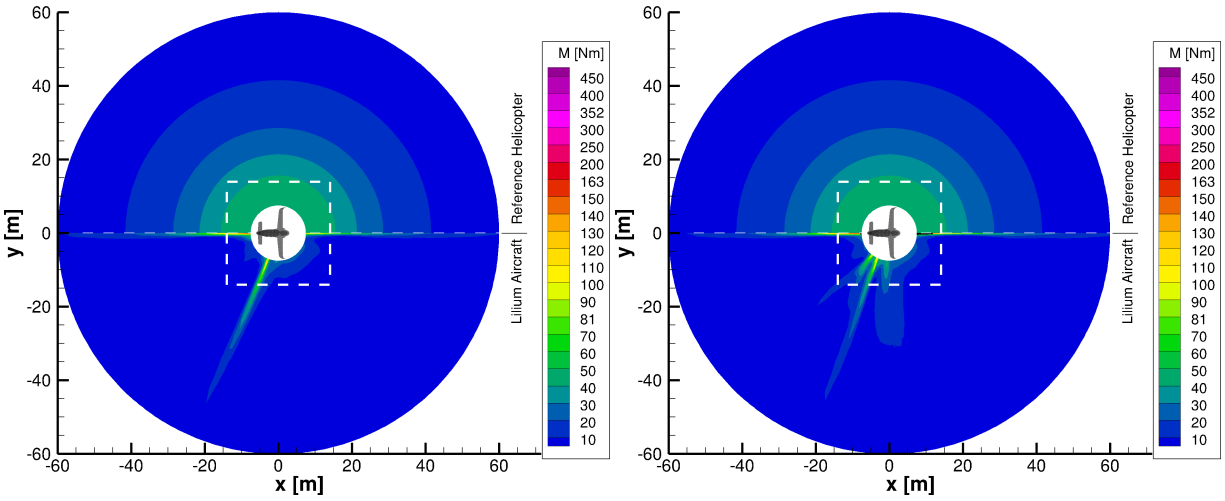

(a) H=18.0 m (b) H=20.0 m

Figure 27: Overturning moment for an adult civilian: results for different hovering heights (3).

11 Appendix B: Additional test cases

It was found that by setting the flap angles so that the canard and main wing jets were angled towards each other by 10° each, and by setting the height of the aircraft, so that the two jets meet at the ground plane (10°), that a stronger 45° jet could be deliberately generated, see Fig. 28. In this case, which as far as we know does not represent a real trim point, the sideward jet would exceed the civilian force limits within the boundary of the clear area around the landing pad, but not outside it. Similarly, the potential for objects to be lifted in a sideward direction exists. Although this combination appears extremely unlikely, it emphasizes that while the qualitative description of the flow appears well defined for hover, that there is a small remaining risk which should be investigated by measurements in the wake once a production-similar aircraft is flying. In contrast, Fig. 29 shows the outflow if all else is left the same and the canard and wing jets are angled away from each other by 10° each. This leads to a qualitatively similar result to the hover test cases in Appendix A, with no danger to civilians outside the boundary of the clear area around the landing pad.

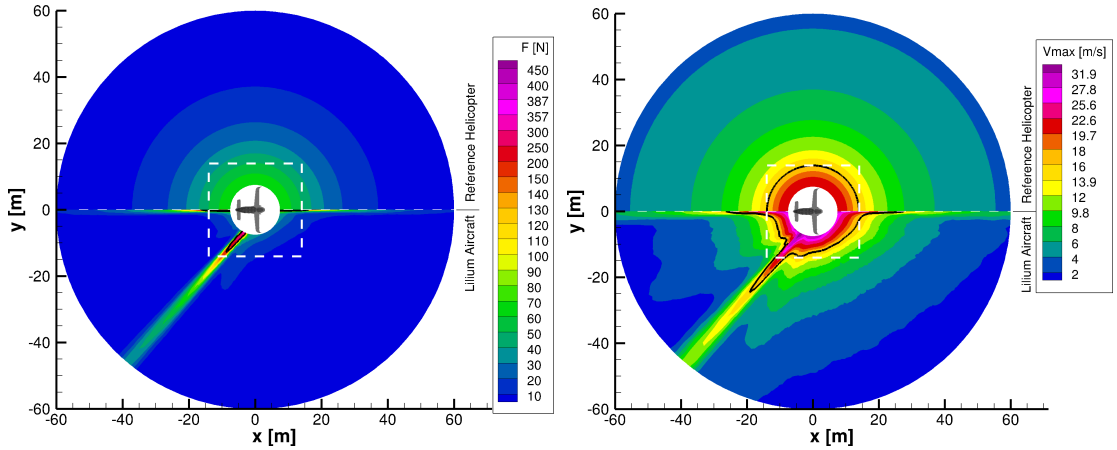

Figure 28: Contours for hover height 10 m with the wing and canard flaps each pointed 10° **toward** each other. Left: PAXMAN, Right: V_{max}.

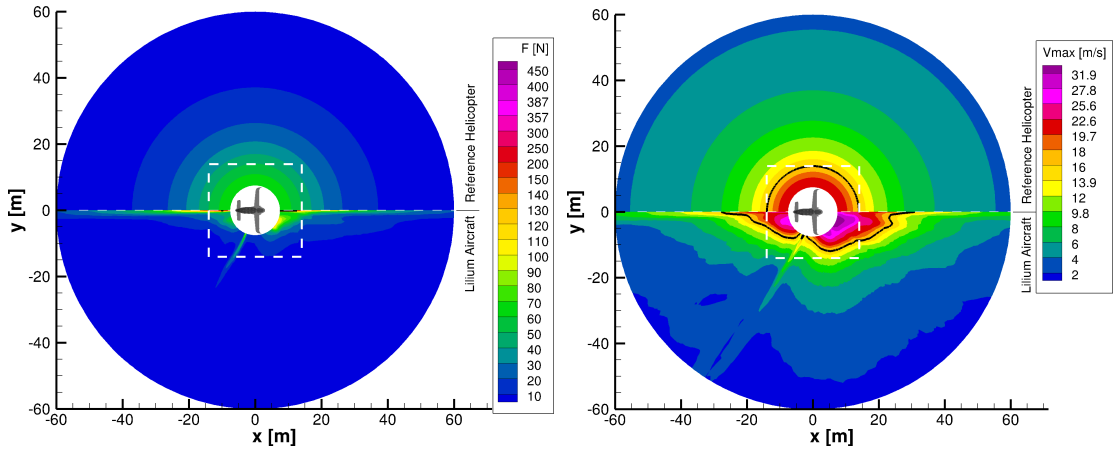

Figure 29: Contours for hover height 10 m with the wing and canard flaps each pointed 10° **away from** each other. Left: PAXMAN, Right: V_{max}.

If we consider that significant side-wind may move the region of high velocity to the side, it is interesting to investigate the potential effect. Fig. 30 shows the effect of 10 m/s (19.4 kt/ 36 km/h) wind from top to bottom. Here the Lilium jet result is compared with the hovering helicopter with no wind. It can be seen that the high-speed portion of the wake is moved sideward, but that even for this strong wind that the PAXMAN limits are not exceeded outside of the safety area denoted by the white dashed line.

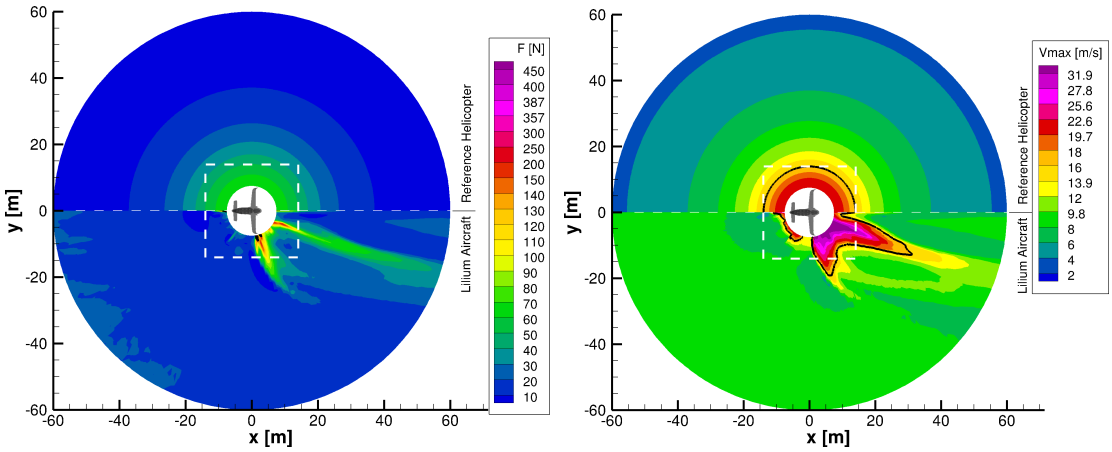

Figure 30: Contours for hover height 10 m with sidewind 10 m/s. Left: PAXMAN, Right: V_{max}.